

**Table II.** Spin-Spin Coupling Constants for Representative PhDBP and Ph<sub>3</sub>P Complexes

compd <sup>a</sup>	<sup>1</sup> J( <sup>199</sup> M- <sup>31</sup> P), Hz	temp, K
(PhDBP) <sub>2</sub> HgI <sub>2</sub>	2217	243
(Ph <sub>3</sub> P) <sub>2</sub> HgI <sub>2</sub> <sup>b</sup>	3073	230
	2951	243
(PhDBP) <sub>2</sub> Hg(SCN) <sub>2</sub>	3001	223
(Ph <sub>3</sub> P) <sub>2</sub> Hg(SCN) <sub>2</sub> <sup>b</sup>	3716	230
(PhDBP) <sub>2</sub> PtCl <sub>2</sub>	3489	299
(Ph <sub>3</sub> P) <sub>2</sub> PtCl <sub>2</sub> <sup>c</sup>	3676	299
(PhDBP)Mo(CO) <sub>5</sub>	132	298
(Ph <sub>3</sub> P)Mo(CO) <sub>5</sub> <sup>d</sup>	139	298
(PhDBP)W(CO) <sub>5</sub>	231	298
(Ph <sub>3</sub> P)W(CO) <sub>5</sub> <sup>e</sup>	245	298

<sup>a</sup> Measured in CH<sub>2</sub>Cl<sub>2</sub> solution. Satisfactory elemental analyses were obtained for the new PhDBP complexes; details of their syntheses will be reported elsewhere. <sup>b</sup> Reference 18. <sup>c</sup> Goel, R. G. *Inorg. Nucl. Chem. Lett.* 1979, 15, 437. <sup>d</sup> Reference 21. <sup>e</sup> Keiter, R. L.; Vander Velde, D. G. *J. Organomet. Chem.* 1983, 258, 234.

The significantly larger coupling constant observed for the PPh<sub>3</sub>AgPF<sub>6</sub> complex indicates that PPh<sub>3</sub> forms a stronger bond to the silver atom than does PhDBP when only PF<sub>6</sub> is a competing ligand. On the other hand, the nearly identical coupling constants for each pair of [(R<sub>3</sub>P)<sub>n</sub>Ag]<sup>+</sup>PF<sub>6</sub><sup>-</sup> (n = 2-4) complexes suggest that PhDBP and Ph<sub>3</sub>P have very similar donor strengths. Together, these observations imply that the lower basicity of PhDBP (pK<sub>a</sub> = 0.5)<sup>15</sup> as compared to that of Ph<sub>3</sub>P (pK<sub>a</sub> = 2.73)<sup>16</sup> is somewhat compensated for by a greater π-acceptor ability for PhDBP. This is supported by the coupling constant data given in Table II for other metal complexes of PhDBP and Ph<sub>3</sub>P. By way of comparison, we have also observed the <sup>31</sup>P NMR spectra for the species R<sub>3</sub>PAgPF<sub>6</sub> and [(R<sub>3</sub>P)<sub>2</sub>Ag]<sup>+</sup>PF<sub>6</sub><sup>-</sup>: R<sub>3</sub>P = (p-CIC<sub>6</sub>H<sub>4</sub>)<sub>3</sub>P (pK<sub>a</sub> = 1.03)<sup>17</sup> and (p-CH<sub>3</sub>OC<sub>6</sub>H<sub>4</sub>)<sub>3</sub>P (pK<sub>a</sub> = 4.57).<sup>17</sup> The coupling constants of 505 and 506 Hz for these two [(R<sub>3</sub>P)<sub>2</sub>Ag]<sup>+</sup>PF<sub>6</sub><sup>-</sup> species differ very little from those observed for the PhDBP and Ph<sub>3</sub>P analogues. The coupling constants of 757 and 767 Hz for these R<sub>3</sub>PAgPF<sub>6</sub> complexes are close to the value observed for PPh<sub>3</sub>AgPF<sub>6</sub>.

It is clear from the data in Figure 1 that the low-coordination-number species persist at relatively higher ligand to metal ratios for PhDBP than for Ph<sub>3</sub>P. For example, the R<sub>3</sub>PAgPF<sub>6</sub> species is still present when the relative L:M ratio is greater than 2.0 for PhDBP. In contrast, the [(R<sub>3</sub>P)<sub>4</sub>Ag]<sup>+</sup>PF<sub>6</sub><sup>-</sup> complex is already present at a L:M ratio of 3.0 for PPh<sub>3</sub>. At the same equivalents added of 2.5 equiv, it is seen that [(Ph<sub>3</sub>P)<sub>2</sub>Ag]<sup>+</sup>PF<sub>6</sub><sup>-</sup> and [(Ph<sub>3</sub>P)<sub>3</sub>Ag]<sup>+</sup>PF<sub>6</sub><sup>-</sup> are present in nearly equal concentrations, whereas only the 1:1 and 1:2 species are present in the solution containing added PhDBP. In addition, the <sup>31</sup>P coordination chemical shifts Δδ<sub>31P</sub> = δ<sub>31P</sub>(complex) - δ<sub>31P</sub>(ligand) (a reasonable measure of metal-phosphorus bond strength) are uniformly larger for the Ph<sub>3</sub>P complexes than for their DPB analogues. Hence, the higher coordination number species have a greater thermodynamic stability for Ph<sub>3</sub>P than for PhDBP. This is surprising as PhDBP is sterically smaller than Ph<sub>3</sub>P. It is interesting to note that the [(R<sub>3</sub>P)<sub>2</sub>Ag]<sup>+</sup>PF<sub>6</sub><sup>-</sup> species for both ligands are fairly stable. They do not disproportionate to higher and lower coordination number species even upon an increase to room temperature. This is perhaps related to the C-P-C bond angle maximization mentioned above for the [(R<sub>3</sub>P)<sub>2</sub>Ag]<sup>+</sup>PF<sub>6</sub><sup>-</sup> species.

Evidence for the faster exchange rate of the PhDBP complexes has already been alluded to in the above discussion. In addition, we note that the line widths of the <sup>31</sup>P resonances for the Ph<sub>3</sub>P complexes are narrower than those of the PhDBP analogues. Also, there are never more than two species present in solution for the Ph<sub>3</sub>P system, whereas three species are simultaneously present for at least three L:M ratios for the PhDBP system. The ease

of formation of [Ag(PhDBP)<sub>4</sub>]<sup>+</sup>PF<sub>6</sub><sup>-</sup> at 223 K (vide infra), even with a deficiency of added PhDBP, similarly is consistent with faster exchange for the phosphole ligand. Thus, in general, the PhDBP complexes are kinetically more labile than the Ph<sub>3</sub>P complexes.

The stepwise additions of either ligand to AgPF<sub>6</sub> solutions at the higher temperature of 223 K again show the presence of four species in each case. Faster exchange is especially evident for both [AgL<sub>3</sub>]<sup>+</sup>PF<sub>6</sub><sup>-</sup> species, and the coupling is not resolved for the broad doublets observed at 2.3 and 11.1 ppm for L = PhDBP and Ph<sub>3</sub>P, respectively. For the Ph<sub>3</sub>P additions, the broad resonance (Δν<sub>1/2</sub> = 470 Hz) at 7 ppm for a 3.5:1 ratio of Ph<sub>3</sub>P to AgPF<sub>6</sub>, which signifies an exchange between Ag(PPh<sub>3</sub>)<sub>3</sub><sup>+</sup> and Ag(PPh<sub>3</sub>)<sub>4</sub><sup>+</sup> cations, changes to a doublet at 5.5 ppm due to Ag(PPh<sub>3</sub>)<sub>4</sub><sup>+</sup> itself with the addition of another 0.5 equiv of Ph<sub>3</sub>P. In contrast, the presence of a resolved doublet of doublets for [Ag(PhDBP)<sub>4</sub>]<sup>+</sup>PF<sub>6</sub><sup>-</sup> at -1.3 ppm is already dominant at a 2.0:1 ratio of PhDBP to AgPF<sub>6</sub>; above a ratio of 2.5:1, only [Ag(PhDBP)<sub>4</sub>]<sup>+</sup>PF<sub>6</sub><sup>-</sup> is observable until excess PhDBP (4.25:1 ratio) gives a peak at -12 ppm. Clearly, PhDBP has a much greater tendency than Ph<sub>3</sub>P to form the higher coordination number species at 223 K.

A correlation between anion electronegativity and J(<sup>199</sup>Hg-<sup>31</sup>P) is expected for mercury(II) phosphine complexes,<sup>18,19</sup> which is consistent with no π-bonding being involved in the mercury-phosphorus bond.<sup>20</sup> The lower <sup>1</sup>J(<sup>199</sup>Hg-<sup>31</sup>P) values for the mercury(II) complexes of PhDBP thus directly reflect the lower σ-donor ability of PhDBP as compared to that of Ph<sub>3</sub>P. If the metal can participate in π-bonding, as is expected for Pt(II), Mo(0), and W(0), then the coupling constants are similar but remain smaller for PhDBP than for Ph<sub>3</sub>P. This is due to the much better π-acceptor ability of PhDBP and the synergistic relation between the σ and π metal-ligand interactions. In corroboration of this property of PhDBP, the <sup>95</sup>Mo NMR chemical shift for (PhDBP)Mo(CO)<sub>5</sub>, -1795 ppm, is considerably upfield from that previously reported for Ph<sub>3</sub>PMo(CO)<sub>5</sub>, -1743 ppm.<sup>21</sup>

Several series of metal complexes are under current investigation in order to compare the coordination chemistry of PhDBP and Ph<sub>3</sub>P in greater detail. The results of these studies will be reported in future publications.

**Acknowledgment.** E.C.A. thanks NSERC Canada for an operating grant and M. Miller, R. Rice, and Z. Wasik for preparation of PhDBP complexes. NMR spectra were obtained on Bruker WH-400 and AM-250 spectrometers at the Southwestern Ontario NMR Centre and at the Waterloo campus of (GWC)<sup>2</sup>, respectively. J.H.N. thanks the donors of the Petroleum Research Fund, administered by the American Chemical Society, for financial support and S. Affandi for the preparation of PhDBP.

(18) Aleya, E. C.; Dias, S. A.; Goel, R. G.; Ogini, W. O.; Pilon, P.; Meek, D. W. *Inorg. Chem.* 1978, 17, 1697.

(19) Allman, T.; Lenkinski, R. E. *Inorg. Chem.* 1986, 25, 3202.

(20) Pidcock, A. In *Transition Metal Complexes of Phosphorus, Arsenic and Antimony Ligands*; McAuliffe, C. A. Ed.; Macmillan: London, 1973; p 1.

(21) Aleya, E. C.; Lenkinski, R. E.; Somogyvari, A. *Polyhedron* 1982, 1, 130.

Contribution from the Department of Chemistry and MSU Shared Laser Laboratory, Michigan State University, East Lansing, Michigan 48824

### Iron Porphyrin π Cation Radicals: Solution Resonance Raman Spectra of (OEP<sup>•+</sup>)Fe<sup>III</sup>(X)(X')

Asaad Salehi, W. Anthony Oertling, Gerald T. Babcock,\* and Chi K. Chang\*

Received July 28, 1987

Heme catalysis in peroxidases, catalases, and cytochromes P450 proceeds through high-valent intermediates, some of which are

(15) Quin, L. D.; Bryson, J. G.; Moreland, C. G. *J. Am. Chem. Soc.* 1969, 91, 3308.

(16) Streuli, C. A. *Anal. Chem.* 1960, 32, 985. Henderson, W. A.; Streuli, C. A. *J. Am. Chem. Soc.* 1960, 82, 5791.

(17) Allman, T.; Goel, R. G. *Can. J. Chem.* 1982, 60, 716.

likely to be oxidized at the porphyrin macrocycle as well as at the central iron.<sup>1</sup> An understanding of the role of these species in the enzymatic cycle requires insight into the interplay between the oxidation state, geometry, and electron density distribution of the porphyrin ring and the valence, spin, and ligation states of the iron.<sup>2</sup> Raman spectroscopy is potentially able to provide this kind of information, and recently we demonstrated its utility in the detection of porphyrin-centered oxidation.<sup>3</sup> This work, however, was confined to metals (i.e., Co, Cu, and Zn) in which the spin state remains intact upon variation in the ring oxidation and metal ligation states. Characterization of oxidized iron porphyrins, on the other hand, covers a wider range of variables owing to several oxidation, ligation, and spin states that are available to the iron atom and has not yet been achieved by Raman spectroscopy.<sup>4</sup>

To address this problem, we report here the solution RR characterization of iron(III) octaethylporphyrin cation radicals of general formula  $(\text{OEP}^{+\bullet})\text{Fe}^{\text{III}}(\text{X})(\text{X}')$ , where  $\text{X} = \text{ClO}_4^-$ ,  $\text{Cl}^-$  and  $\text{X}' = \text{ClO}_4^-$ ,  $\text{SbCl}_6^-$ . We focus on the determination of the solution coordination number and spin state of the iron atom in the porphyrin radicals, as monitored by high-frequency ( $1450\text{--}1700\text{ cm}^{-1}$ ) vibrational modes that are sensitive to porphyrin core conformation. Our data demonstrate the utility of Raman spectroscopy in characterizing iron porphyrin radicals and indicate a preference for the five-coordinate state in solution, at least for the ligand combinations used here. We discuss our results in light of recent NMR, crystal structure, magnetic, and IR data available on the related tetraphenylporphyrin (TPP) derivatives.

### Experimental Section

**Instrumentation.** UV-vis spectra were recorded by using a Cary 219 spectrophotometer. The 363.8- and 351.1-nm lines used to record the RR spectra were obtained from a Coherent Innova 100-20 argon ion laser; the Raman equipment is described in detail elsewhere.<sup>3c</sup> Magnetic susceptibility measurements were performed on an SHE SQUID susceptometer at a field of 5 kG.

**Chemical Oxidations.** Typically, samples were prepared at room temperature in dry  $\text{CH}_2\text{Cl}_2$  by using a slight stoichiometric excess of the oxidant, according to the published reports.<sup>2a,5</sup> The progress of the reaction was followed spectrophotometrically until complete oxidation was achieved.  $(\text{OEP}^{+\bullet})\text{Fe}^{\text{III}}(\text{ClO}_4)_2$  (**1**) was prepared from  $[(\text{OEP})\text{Fe}]_2\text{O}$  by using  $\text{Fe}(\text{ClO}_4)_3 \cdot x\text{H}_2\text{O}$  (yellow) in the presence of trace  $\text{HClO}_4$  to assist in the breaking of the  $\mu$ -oxo bridge of the dimer. UV-vis for **1** ( $\text{CH}_2\text{Cl}_2$ ;  $\lambda_{\text{max}}$ , nm ( $10^{-3}\epsilon$ ): 357 (86), 517 (14.5), 578 (broad).  $\mu_{\text{eff}} = 6.7 \mu_{\text{B}}$  (solid state, 300 K).  $(\text{OEP}^{+\bullet})\text{Fe}^{\text{III}}(\text{Cl}^-)(\text{SbCl}_6^-)$  (**2**) was prepared from  $(\text{OEP})\text{FeCl}$  by using phenoxathiin hexachloroantimonate as the oxidant.<sup>2c</sup> UV-vis for **2** ( $\text{CH}_2\text{Cl}_2$ ;  $\lambda_{\text{max}}$ , nm ( $10^{-3}\epsilon$ ): 357 (84), 519 (14.7).  $\mu_{\text{eff}} = 5.2 \mu_{\text{B}}$  (solid state, 300 K).

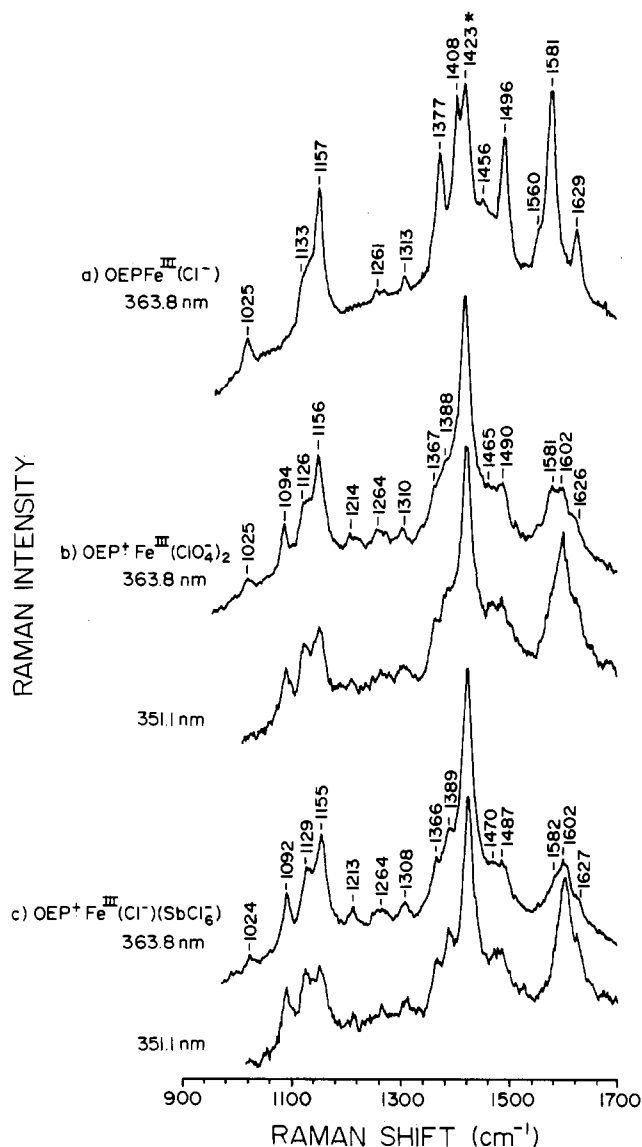


**Figure 1.** Near-UV RR spectra of  $(\text{OEP}^{+\bullet})\text{Fe}^{\text{III}}(\text{X})(\text{X}')$  complexes. The laser power was 35–40 mW. The solvent ( $\text{CH}_2\text{Cl}_2$ ) band at  $1423\text{ cm}^{-1}$  is labeled with an asterisk.

The integrity of the samples was verified by monitoring the absorption spectra before and after the RR spectra. The choice of the excitation line, however, is of importance to minimize contributions from ferric porphyrin and diacid salt contaminations,<sup>3b</sup> which may be difficult to observe in the optical spectra, and to select predominantly for the porphyrin radical.

### Results and Discussion

Our magnetic susceptibility data for **1** ( $\mu_{\text{eff}} = 6.7 \mu_{\text{B}}$ ) and **2** ( $\mu_{\text{eff}} = 5.2 \mu_{\text{B}}$ ) show that the effective magnetic moment for ferric OEP  $\pi$  cation radicals in the solid state is a function of the axial ligation. A similar dependence occurs for solid-state ferric TPP radicals, as  $(\text{TPP}^{+\bullet})\text{Fe}^{\text{III}}(\text{ClO}_4)_2$  (**3**) has  $\mu_{\text{eff}} = 6.5 \mu_{\text{B}}$  while  $(\text{TPP}^{+\bullet})\text{Fe}^{\text{III}}(\text{Cl}^-)(\text{SbCl}_6^-)$  (**4**) has  $\mu_{\text{eff}} = 4.8 \mu_{\text{B}}$ .<sup>6</sup> The latter data have been rationalized by X-ray crystallographic work.<sup>6,7</sup> **3** has a planar core with both perchlorate ions ligated to the iron; this geometry apparently leads to strong ferromagnetic coupling between the high-spin ferric ion and the ring-centered radical to

- (a) Edwards, S. L.; Xuong, N. H.; Hamlin, R. C.; Kraut, J. *Biochemistry* **1987**, *26*, 1503–1511. (b) Hanson, L. K.; Chang, C. K.; Davis, M. S.; Fajer, J. *J. Am. Chem. Soc.* **1981**, *103*, 663–670. (c) Guengerich, F. P.; MacDonald, T. L. *Acc. Chem. Res.* **1984**, *17*, 9–16.
- (a) Phillippi, M. A.; Goff, H. M. *J. Am. Chem. Soc.* **1982**, *104*, 6026–6034. (b) Phillippi, M. A.; Shimomura, E. T.; Goff, H. M. *Inorg. Chem.* **1981**, *20*, 1322–1325. (c) Gans, P.; Marchon, J.-C.; Reed, C. A.; Regnard, J.-R. *Nouv. J. Chim.* **1981**, *5*, 203–204. (d) Fuhrhop, J. H. *Struct. Bonding (Berlin)* **1974**, *18*, 1–67. (e) Groves, J. T.; Quinn, R.; McMurry, T. J.; Lang, G.; Boso, B. *J. Chem. Soc., Chem. Commun.* **1984**, 1455–1456. (f) Erler, B. S.; Scholz, W. F.; Lee, Y. J.; Scheidt, R.; Reed, C. A. *J. Am. Chem. Soc.* **1987**, *109*, 2644–2652.
- (a) Salehi, A.; Oertling, W. A.; Babcock, G. T.; Chang, C. K. *J. Am. Chem. Soc.* **1986**, *108*, 5630–5631. (b) Oertling, W. A.; Salehi, A.; Chang, C. K.; Babcock, G. T. *J. Phys. Chem.* **1987**, *91*, 3114–3116. (c) Oertling, W. A.; Salehi, A.; Chung, Y. C.; Leroy, G. E.; Chang, C. K.; Babcock, G. T. *J. Phys. Chem.*, in press.
- (a) Goff, H. M.; Phillippi, M. A. *J. Am. Chem. Soc.* **1983**, *105*, 7567–7571. (b) Lee, W. A.; Calderwood, T. S.; Bruice, T. C. *Proc. Natl. Acad. Sci. U.S.A.* **1982**, *82*, 4301–4305. (c) Balch, A. L.; Lantos-Grazynski, L.; Renner, M. W. *J. Am. Chem. Soc.* **1985**, *107*, 2983–2985.
- (5) Carnieri, N.; Harriman, A. *Inorg. Chim. Acta* **1982**, *62*, 103–107.
- (6) Gans, P.; Buisson, G.; Duee, E.; Marchon, J.-C.; Erler, B. S.; Scholz, W. F.; Reed, C. A. *J. Am. Chem. Soc.* **1986**, *108*, 1223–1234.
- (7) (a) Scholz, W. F.; Reed, C. A.; Lee, Y. J.; Scheidt, W. R.; Lang, G. *J. Am. Chem. Soc.* **1982**, *104*, 6791–6793. (b) Buisson, G.; Deronzier, A.; Duee, E.; Gans, P.; Marchon, J.-C.; Regnard, J.-R. *J. Am. Chem. Soc.* **1982**, *104*, 6793–6796. (c) Groves, J. T.; Quinn, R.; McMurry, T. J.; Nakamura, M.; Lang, G.; Boso, B. *J. Am. Chem. Soc.* **1985**, *107*, 354–360.

Table I. RR Frequencies ( $\text{cm}^{-1}$ ) of Selected Iron OEP Species

mode	(OEP <sup>2+</sup> )Fe <sup>III</sup> (ClO <sub>4</sub> <sup>-</sup> ) <sub>2</sub> (1)	(OEP <sup>2+</sup> )Fe <sup>III</sup> (Cl <sup>-</sup> )(SbCl <sub>6</sub> <sup>-</sup> ) (2)	(OEP)Fe <sup>III</sup> (Cl <sup>-</sup> ) (5) ( $\Delta\nu$ ) <sup>a</sup>	(OEP)Fe <sup>III</sup> (DMSO) <sub>2</sub> (6) ( $\Delta\nu$ ) <sup>a</sup>	predicted $\Delta\nu_{av}$ <sup>b</sup>
$\nu_{10}(\text{C}_a\text{C}_m)$	1626	1627	1629 (-3)	1615 (+11)	-4
$\nu_2(\text{C}_b\text{C}_b)$	1602	1602	1581 (+21)	1576 (+26)	+20
$\nu_{11}(\text{C}_b\text{C}_b)$	1581	1582	1560 (+21)		+26
$\nu_3(\text{C}_a\text{C}_m)$	1490	1487	1496 (-7)	1483 (+6)	-7

<sup>a</sup> Obtained as the average frequency difference for the indicated mode in the cation radicals and either the neutral five-coordinate species (column 4) or the neutral six-coordinate species (column 5). <sup>b</sup> From ref 3c.

produce an overall spin of  $S = 3$ . Solid-state IR data on **3** and its tetramesitylporphyrin (TMP) analogue are consistent with bisaxial ligation.<sup>7,8</sup> **4**, however, is five-coordinated and exhibits a ruffled core, which presumably leads to antiferromagnetic exchange and a room-temperature  $S = 2$  state.

In solution **4** maintains its five-coordinate ligation geometry. Boersma and Goff, however, have interpreted NMR and magnetic data to suggest that **3** undergoes axial ligand dissociation and also adopts a five-coordinate geometry in solution.<sup>9</sup> Raman spectroscopy of these ferric cation radicals provides an independent means by which to test this suggestion; moreover, such a study will assess the applicability of Raman techniques to characterizing ring-oxidized iron porphyrin species. As in our earlier work, we have focused on iron OEP derivatives owing to their biologically relevant peripheral substitution pattern. The similarity in magnetic moments between Fe<sup>III</sup>OEP cation radicals and Fe<sup>III</sup>TPP cation radicals noted above indicates that the altered pattern of peripheral substitution is unlikely to perturb axial ligation behavior significantly.

Figure 1 shows Raman spectra of **1** and **2** along with that of the five-coordinate ring neutral (OEP)Fe<sup>III</sup>(Cl<sup>-</sup>) species (**5**) in methylene chloride. An assignment of the principal high-frequency modes for these species as well as of (OEP)Fe<sup>III</sup>(DMSO)<sub>2</sub> (**6**)<sup>10</sup> is given in Table I. The frequency differences apparent in comparing corresponding modes for the two ring neutral species, **5** and **6**, are understood and correlate inversely with porphyrin core size. The similarities for **1** and **2** in the frequencies of these modes, which retain core-size sensitivity in the metalloporphyrin

cation radicals,<sup>3c</sup> indicate that the solution geometry for these two radicals is similar, in agreement with the Boersma and Goff suggestion.

We can gain further insight into the coordination state of these radicals by referring to earlier work with valence +2 metalloporphyrin derivatives.<sup>3c</sup> For this class of compounds we showed that vibrational modes with predominantly C<sub>b</sub>C<sub>b</sub> character are  $\sim 20 \text{ cm}^{-1}$  higher in a given radical relative to the corresponding modes in its neutral precursor, whereas those with significant C<sub>a</sub>C<sub>m</sub> character are  $\sim 5 \text{ cm}^{-1}$  lower (Table I, column 6). The physical basis for this behavior lies in the fact that there is little change in porphyrin core geometry upon ring-centered oxidation. This correlation indicates, then, that the axial coordination for the OEP radicals in Figure 1 may be assigned by considering their frequency shifts relative to those for the neutral five- and six-coordinate ferric OEP species. Inspection of Table I shows that the pattern of frequency shifts observed for the valence +2 metalloporphyrin derivatives is reproduced when the ferric  $\pi$  cation radicals are considered to be five-coordinate in solution (column 4); assuming a six-coordinate solution state for the radicals (column 5) produces poor agreement with our earlier data.

Two conclusions follow from these data. First, the porphyrin core geometries of both **1** and **2** in solution are characteristic of a five-coordinate state, consistent with the suggestion that axial ligand dissociation occurs when **2** goes into solution.<sup>9</sup> Second, the pattern of vibrational frequency changes that occurs upon ring oxidation of +2 metalloporphyrin derivatives<sup>3c</sup> appears to hold as well for the more complex, but biologically more relevant, iron porphyrins. At present, we are exploring the applicability of these correlations to iron(IV) porphyrin radicals that model intermediates in the catalytic cycles of several classes of heme protein enzymes.

**Acknowledgment.** This research was supported by NIH Grants GM 25480 (G.T.B.) and GM 36520 (C.K.C.).

(8) *Warning:* Laser irradiation of solid perchlorate salts may cause explosion. Because of this phenomenon, we were unsuccessful in our attempts to measure the RR spectrum of **1** in the solid state.

(9) Boersma, A. D.; Goff, H. M. *Inorg. Chem.* **1984**, *23*, 1671-1676.

(10) Callahan, P. M.; Babcock, G. T. *Biochemistry* **1981**, *20*, 952-958.